EE 445/645: Physical Models in Remote Sensing (Spring 2026)

Chapter 02-Part 01: Vegetation Canopy Structure – Notes (See C2-P1 PPTs)

Prof. Ranga B. Myneni, Boston University

ranga.myneni@gmail.com

§1. Introduction.

The canopies of natural vegetation exhibit a complexity and variability of structure that, in their full particulars, defy precise mathematical description. The intricate arrangement of leaves, branches, stems, and reproductive organs presents a formidable challenge to any attempt at quantitative characterization. Yet the progress of physical remote sensing demands that we construct workable representations of the canopy, for it is through the canopy that electromagnetic radiation must pass on its way from sun to sensor, and it is the structure of the canopy that governs, in large measure, the nature of this passage.

In developing physical models of radiative transfer in vegetation, we adopt an idealization that, while drastic in its simplifications, captures the essential features of the canopy that are most relevant to the exchange of radiant energy. We shall regard the vegetation canopy as a turbid medium—a volume filled with small, flat, planar elements of negligible thickness, distributed throughout the canopy space. This conception, sometimes referred to as the *green gas* approximation, treats the foliage as a statistical ensemble of scattering and absorbing elements, much as the kinetic theory of gases treats molecules as point particles endowed with certain cross sections.

The abstraction ignores all organs of the plant other than the green leaves. It sets aside trunks, branches, bark, flowers, and fruits. This may appear a severe limitation, but it captures the single most significant aspect of the canopy for our purposes: it is the foliage that plays the central role in exchanges of energy, mass, and momentum between the canopy and the overlying atmospheric boundary layer, and it is the foliage that principally governs the reflectance, transmittance, and absorptance of the canopy in the optical and near-infrared portions of the spectrum.

Within this *turbid medium* framework, the complete structural characterization of the vegetation canopy reduces to the specification of two fundamental quantities: the leaf area density, which describes how densely the foliage elements are packed within the canopy volume, and the leaf normal orientation distribution, which describes how these elements are inclined and rotated in three-dimensional space. We shall examine each of these quantities in turn, developing the mathematical formalism that will underpin all subsequent treatments of radiative transfer in vegetation.

§2. Lidar reconstruction of vegetation canopies.

Before proceeding to the mathematical formalism, it is instructive to consider the empirical basis upon which our understanding of canopy structure rests. The advent of lidar—Light Detection and Ranging—has provided a remarkably powerful means of characterizing the three-dimensional structure of vegetation canopies. Airborne or ground-based lidar instruments emit pulses of laser radiation and record the time delay and intensity of the return signals scattered by canopy elements. From these measurements, one may reconstruct a three-dimensional point cloud representing the spatial locations of foliage elements within the canopy (Figure 1).

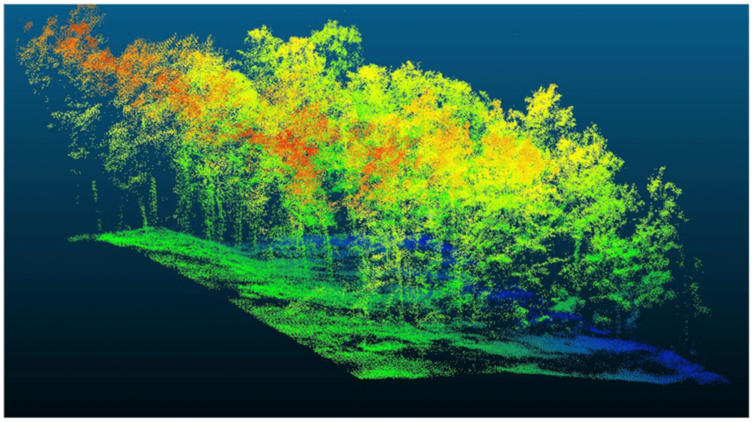

Figure 1. Airborne Laser Scanning (ALS) point cloud. Tile of ALS point cloud showing the heterogeneity of the forest stand structure in Bosco Pennataro in Central Apennine, in Molise Region (Italy) [Santopuoli, G. et al., (2020). Remote Sensing. 12. 1-19. 10.3390/rs12132142].

The reconstructed canopies thus obtained are not merely schematic representations; they accurately capture the spatial distribution of foliage in the canopy space, and they appear visually realistic when rendered. Such reconstructions have proved invaluable in studies of vegetation structure, biomass estimation, carbon accounting, and hydrological modelling.

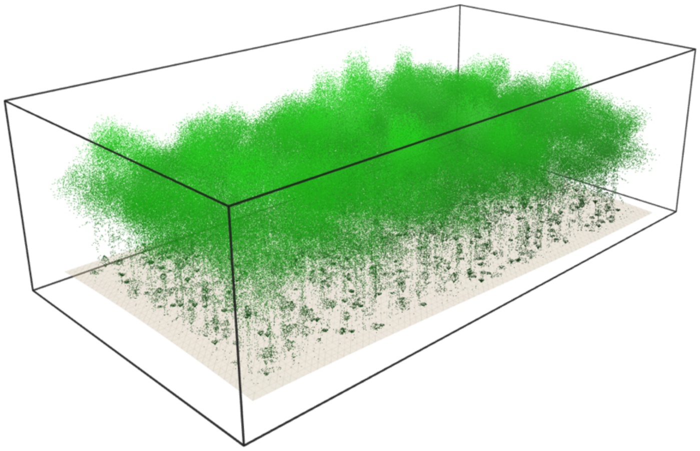

Figure 2. Simulated temperate deciduous forest.

To illustrate the richness of information contained in these lidar-derived representations, consider a simulated temperate forest plot of dimensions 120 × 60 metres, containing 500 individual trees at a density of approximately 700 trees per hectare, drawn from 10 broadleaf deciduous species (Figure 2). The leaf area index of this simulated stand is 3.84, with each individual leaf possessing an area of approximately 0.0411 m². The resulting point cloud comprises 750,000 to

850,000 points, of which roughly 700,000 correspond to leaf positions; the remainder represent other canopy elements.

§3. Leaf area density.

We now introduce the first of our two fundamental structural variables. Let us consider a small volume element within the canopy, centred at the point with position vector **r**. Within this element, we may count the total one-sided area of all leaves. The *leaf area density*, which we shall denote by u_L, is defined as the total one-sided area of leaves per unit volume of the canopy space:

$$u_L(\mathbf{r}) = lim \frac{\Delta S_L}{\Delta V}, \tag{1}$$

where ΔS_L denotes the total one-sided leaf area contained within the volume element ΔV (Figure 3). The leaf area density has dimensions of inverse length (m^{-1}), and it varies, in general, throughout the canopy in all three spatial dimensions.

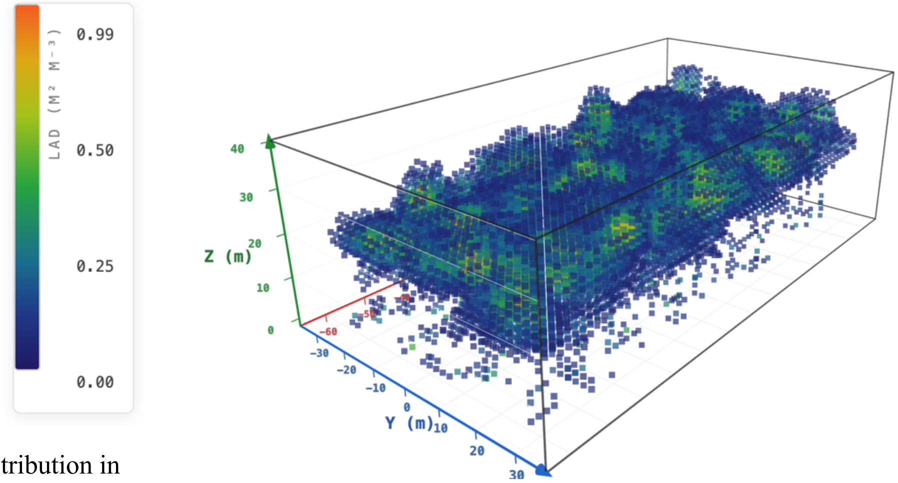

Figure 3. Leaf area density distribution in the simulated temperate forest.

The variation of leaf area density within the canopy reflects the architecture of the vegetation. Near the top of the canopy, where insolation is abundant, trees deploy their foliage densely to intercept the maximum flux of photosynthetically active radiation. In the interior of the canopy, where the light environment is attenuated by the overlying foliage layers, leaf area density typically diminishes. The horizontal variation of leaf area density is governed by the spatial arrangement of individual tree crowns and the gaps between them.

§4. Vertical profile of leaf area density.

Of particular importance for radiative transfer modelling is the vertical profile of leaf area density—that is, the function $u_L(z)$ describing how the leaf area density varies with height z above the ground. In many forest canopies, this profile assumes a characteristic form: the density is low near the ground surface, where the understory may be sparse; it increases through the mid-canopy, where the bulk of the foliage is concentrated; and it tapers to zero at the canopy top (Figure 4).

The precise form of the vertical profile depends upon the tree species, the forest type, the age of the stand, and its management history. In a plantation of uniform species and age, the profile may be sharply peaked; in a natural mixed-species forest with a well-developed understorey, it may exhibit multiple maxima. This profile constitutes a key input to all one-dimensional models of canopy radiative transfer, for it determines the rate at which radiation is attenuated as it penetrates downward through the canopy layers.

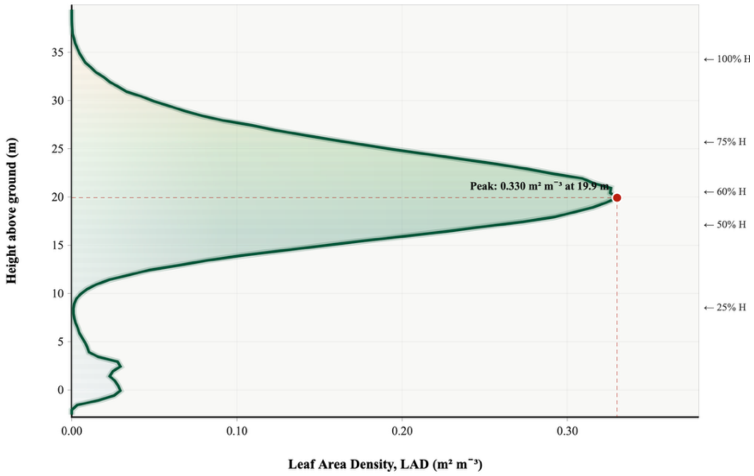

Figure 4. Vertical profile of leaf area density distribution in the simulated temperate forest.

§5. Leaf area index.

Closely related to the leaf area density is the *leaf area index*, universally denoted by L (or LAI in the remote sensing literature). The leaf area index is defined as the total one-sided leaf area per unit ground surface area. It may be obtained from the leaf area density by vertical integration over the entire depth of the canopy:

$$L = \int_0^H u_L(z) dz, \tag{2}$$

where H denotes the total height of the canopy (Figure 5a). The leaf area index is dimensionless, being a ratio of area to area. A value of $L = 1$ signifies that the total leaf area, if spread uniformly upon the ground, would cover the ground surface exactly once.

In nature, the leaf area index ranges from values well below unity in sparse grasslands and arid shrublands to values of 6 or more in dense tropical forests. The leaf area index is, perhaps, the single most widely measured and modelled variable in the remote sensing of vegetation. It serves as a critical input to models of photosynthesis, evapotranspiration, precipitation interception, and carbon cycling.

§6. Global distribution of leaf area index.

The capacity of satellite remote sensing to map the leaf area index over the entire terrestrial surface of the Earth constitutes one of the notable achievements of the discipline. The Moderate

Resolution Imaging Spectroradiometer (MODIS), carried aboard the Terra and Aqua satellites, provides measurements of surface reflectance from which the leaf area index may be retrieved at a spatial resolution of approximately one kilometre.

The global distribution of annual average vegetation green leaf area index $L(x, y)$ at 1 km resolution derived from MODIS measurements reveals the expected geographical patterns. The tropical rainforests of the Amazon basin, equatorial Africa, and Southeast Asia exhibit the highest values; the temperate forests of North America, Europe, and East Asia display moderate values; and the arid and semi-arid regions—the Sahara, the Arabian Peninsula, central Australia—show values approaching zero.

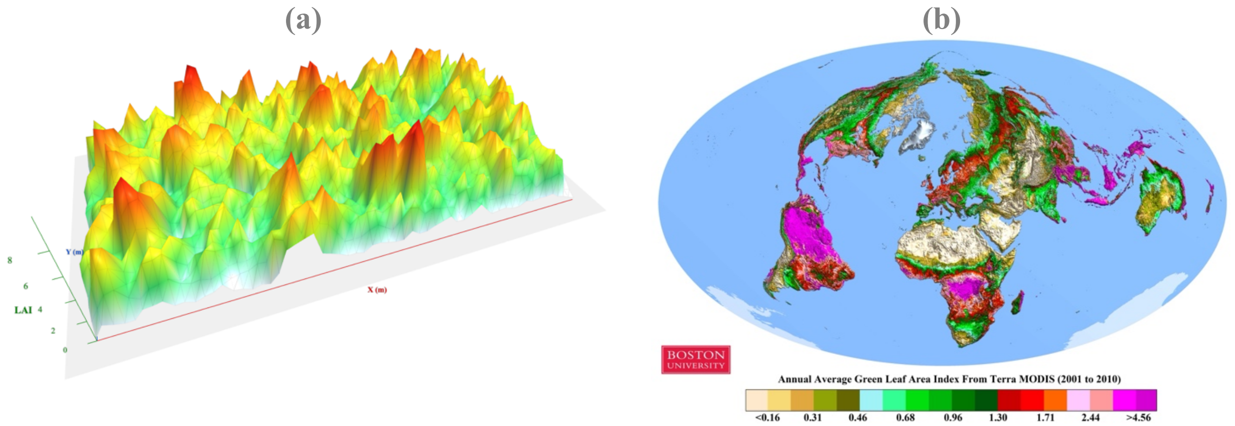

Figure 5. **(a)** Spatial distribution of LAI in the simulated temperate forest. **(b)** Global distribution of annual average vegetation green leaf area index *L(x,y)* at 1 km resolution derived from MODIS measurements of surface reflectances.

§7. The leaf normal distribution function.

We now turn to the second fundamental quantity required for the characterization of the vegetation canopy as a turbid medium: the distribution of leaf orientations in three-dimensional space. Every leaf in the canopy possesses a surface whose orientation may be described by its outward-pointing unit normal vector. The *leaf normal distribution function* describes the probability density of leaf normal orientations across the entire foliage ensemble.

Let us denote the leaf normal direction by the pair of angles (θ_L, φ_L), where θ_L is the inclination (zenith) angle measured from the vertical, and φ_L is the azimuthal angle measured in the horizontal plane (Figure 6). The leaf normal distribution function, which we write as $g_L(\theta_L, \varphi_L)$, is normalized so that

$$\frac{1}{2\pi}\int_0^{2\pi}\int_0^{\pi/2} g_L(\theta_L, \varphi_L)\sin\theta_L\, d\theta_L\, d\varphi_L = 1. \tag{3}$$

The significance of the leaf normal distribution for remote sensing cannot be overstated. The orientation of a leaf relative to the direction of incident solar radiation and the sensor viewing direction determines what fraction of the leaf surface is illuminated, and what fraction is visible to the sensor. A canopy composed predominantly of horizontal leaves interacts with the radiation field very differently from one composed of vertical leaves.

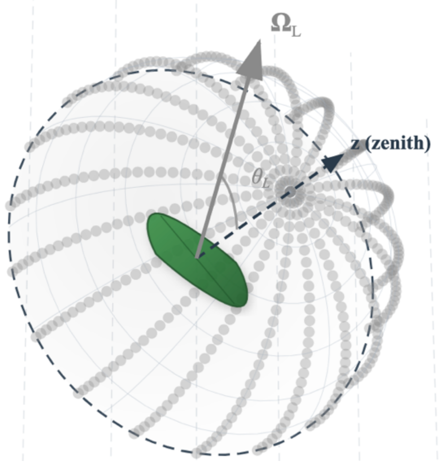

Figure 6. Geometry of leaf normal orientation.

§8. The inclination and azimuthal distribution functions.

It proves convenient, and is physically well motivated, to decompose the full leaf normal distribution function into the product of an inclination distribution and an azimuthal distribution:

$$g_L(\theta_L, \varphi_L) = \overline{g_L}(\theta_L) \cdot h_L(\varphi_L), \tag{4}$$

where $\overline{g_L}(\theta_L)$ is the *leaf normal inclination distribution function*, describing the probability density of the zenith angle of the leaf normal, and $h_L(\varphi_L)$ is the *leaf normal azimuthal distribution function*, describing the probability density of the compass direction in which the leaf normal is oriented. These functions satisfy, respectively,

$$\int_0^{\pi/2} \overline{g_L}(\theta_L) \sin\theta_L \, d\theta_L = 1, \tag{5}$$

and

$$\frac{1}{2\pi}\int_0^{2\pi} h_L(\varphi_L) \, d\varphi_L = 1. \tag{6}$$

In the great majority of natural canopies, the azimuthal distribution is approximately uniform—that is, leaves face all compass directions with roughly equal probability. This uniformity obtains whenever the canopy is not subject to a dominant directional influence such as a persistent wind or a slope-induced solar geometry.

When the azimuthal distribution is uniform, $h_L(\varphi_L) = 1$, and the full distribution function reduces to the inclination distribution alone. The inclination distribution is the more consequential of the two components for the interaction of radiation with vegetation, and we devote the next several sections to its description.

§9. Models for the leaf normal inclination distribution function.

Several mathematical models have been proposed to describe the distribution of leaf inclination angles within vegetation canopies. These models furnish analytical expressions for the function that gives the probability density of leaf normals as a function of the inclination angle. Though idealized, they capture the principal patterns observed in the natural world.

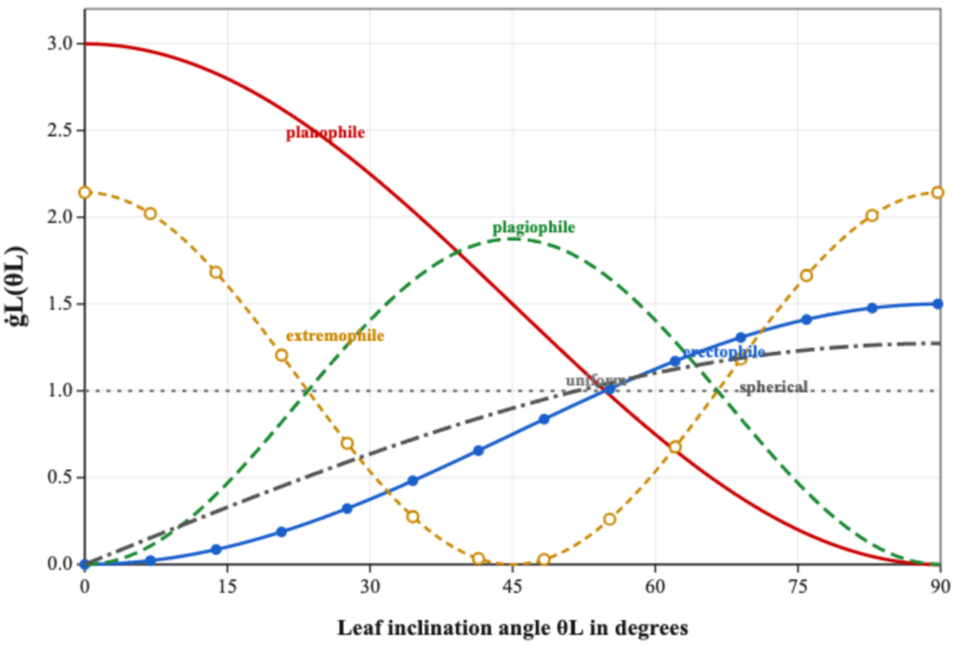

Figure 7. Models for leaf normal inclination distribution function.

Seven canonical forms are commonly distinguished (Figure 7). These models are slightly different than those conventionally used, but as probability density functions they satisfy the normalization in Eq. (5).

(i) *Uniform.* In the uniform distribution, all inclination angles from 0 to $\pi/2$ are equally probable. We have $\bar{g}_L(\theta_L) = 1$. Leaves are as likely to be horizontal as vertical or inclined at any intermediate angle. No preference is accorded to any particular orientation.

(ii) *Planophile.* In the planophile distribution, the foliage is predominantly horizontal: $\bar{g}_L(\theta_L) = 3\cos^2\theta_L$. The function $\bar{g}_L$ is concentrated at small values of θ_L, corresponding to nearly horizontal leaves whose normals point close to the vertical. This distribution is characteristic of shade-adapted species in the forest understorey, where maximising the interception of the attenuated downwelling radiation is advantageous.

(iii) *Erectophile.* The erectophile distribution is the antithesis of the planophile: $\bar{g}_L(\theta_L) = \frac{3}{2}\sin^2\theta_L$. Leaves are predominantly erect, with normals concentrated near the horizontal direction (large θ_L). This arrangement is commonly observed in grasses and cereal crops, where the vertical orientation of the leaf blades permits solar radiation to penetrate deeply into the canopy, distributing the light more uniformly among the leaves.

(iv) *Plagiophile.* In the plagiophile distribution, the predominant leaf inclination is near 45°: $\bar{g}_L(\theta_L) = \frac{15}{8}\sin^2 2\theta_L$. The function $\bar{g}_L$ peaks in the neighbourhood of $\theta_L = \pi/4$. This intermediate orientation represents a compromise between the competing demands of light interception and light penetration.

(v) *Extremophile.* The extremophile distribution is bimodal: $\bar{g}_L(\theta_L) = \frac{15}{7}\cos^2 2\theta_L$. Leaves are concentrated at the two extremes of the angular range — some nearly horizontal, others nearly vertical — with relatively few at intermediate angles. This distribution is of theoretical interest as a limiting case.

(vi) *Spherical.* In the spherical distribution, the leaf inclination angle θ_L is uniformly distributed over $[0, \pi/2]$ with respect to the flat measure $d\theta_L$: $\bar{g}_L(\theta_L) = \frac{4}{\pi}\sin\theta_L$. Because the solid-angle element on the hemisphere is proportional to $\sin\theta_L$, a distribution that is uniform in θ_L itself requires $\bar{g}_L$ to increase with θ_L, weighting near-vertical leaf orientations (large θ_L) more heavily than the isotropic (uniform) case.

(vii) *Constant.* In this case, all leaf normals are assumed to have a single fixed inclination. Thus $\bar{g}_L(\theta_L) = \delta(\theta_L - \theta_0)/\sin\theta_0$, where δ is the Dirac delta function and the factor $1/\sin\theta_0$ ensures proper normalisation with respect to the solid-angle measure $\sin\theta_L \, d\theta_L$. The special cases of purely horizontal and purely vertical foliage correspond to $\theta_0 = 0$ and $\theta_0 = \pi/2$, respectively.

§10. Models for the leaf normal azimuthal distribution function.

We have noted that, in the majority of natural canopies, the azimuthal distribution of leaf normals is approximately uniform. There exist, however, situations in which the leaves exhibit a preferential azimuthal orientation. Heliotropic species, for example, orient their leaves to track the sun; paraheliotropic species orient their leaves to minimize direct solar incidence. For such canopies, the function $h_L(\varphi_L)$ departs from unity and must be modelled explicitly.

A simple model for $h_L(\varphi_L)$ is,

$$\frac{1}{2\pi}\, h_L(\varphi_L,\varphi) = \frac{1}{\pi}\, cos^2(\varphi - \varphi_L - \eta)\,, \tag{7}$$

where η is the difference between the azimuth of the maximum of the distribution function $h_L$and the solar azimuth. Two forms of this model are: Diaheliotropic: maximize the projected leaf area to the incident photon stream, $\eta = 0$, and Paraheliotropic: minimize the projected leaf area to the incident photon stream, $\eta = 0.5\pi$.

A convenient parameterization employs a truncated Fourier series in the azimuthal angle. The simplest non-uniform model adds a single cosine term, allowing for a preferred azimuthal direction with a prescribed degree of anisotropy. The parameters of such models may be fitted to field measurements of leaf orientation obtained by direct sampling or by stereo-photographic techniques.

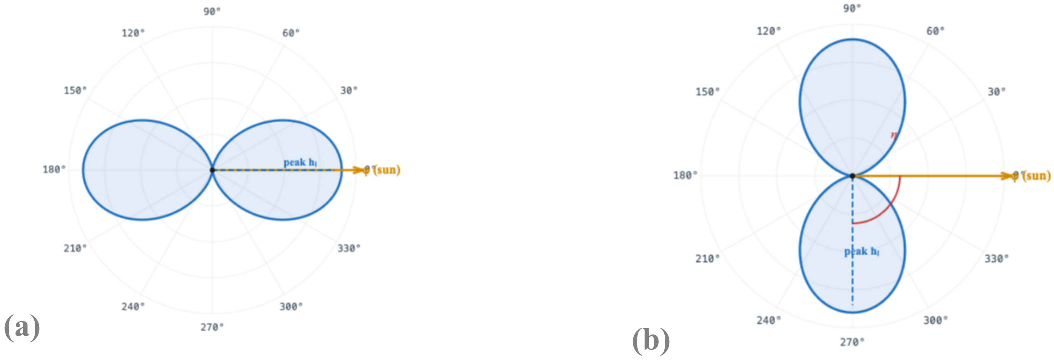

Figure 8. **(a)** Diaheliotropic and **(b)** Paraheliotropic leaf normal azimuthal distribution functions.

§11. The case of needle canopies.

The foregoing development has been predicated upon the assumption that foliage elements are flat, planar objects—an assumption well suited to the broad leaves of deciduous trees and many herbaceous species, but one that requires modification when applied to the needles of coniferous trees. The needles of pines, spruces, firs, *etc*. are long, slender, and approximately cylindrical. For such elements, the notion of a single leaf normal is not straightforwardly defined, since the surface of a cylinder has normals pointing in every direction perpendicular to the cylinder axis.

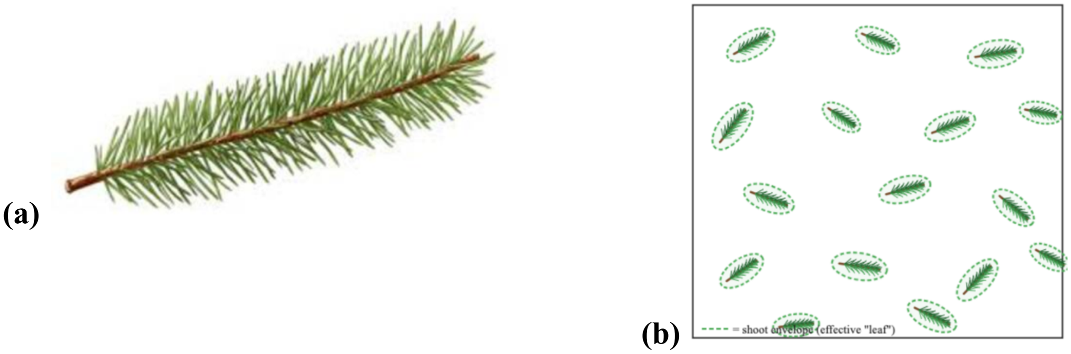

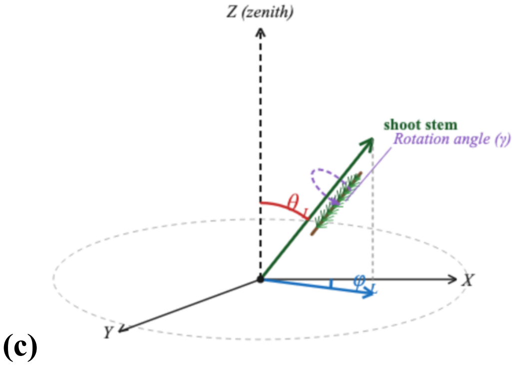

Figure 9. **(a)** A pine shoot. **(b)**. Abstraction of a shoot with needles as a broadleaf. **(c)** Geometry of shoot orientation.

For needle-like foliage elements, we characterize the orientation by the direction of the shoot axis rather than by a surface normal. The cross-sectional area that the shoot presents to a beam of radiation coming from a given direction must then be computed from the geometry of a cylinder rather than a flat plate. Let the shoot axis be oriented in the direction specified by the zenith and azimuthal angles of the axis. The projected area of a cylindrical element of length and diameter, as seen from the direction of the incident beam, depends upon the angle between the beam direction and the shoot axis.

The mathematical treatment of needle canopies thus requires a modification of the projection function—the function that relates the orientation distribution of the foliage to the effective cross-sectional area presented to a beam from a given direction. For flat leaves, the projection function depends on the cosine of the angle between the leaf normal and the beam direction. For needles, it depends instead on the sine of the angle between the shoot axis and the beam direction, integrated over the azimuthal symmetry of the cylinder. This distinction has important consequences for the transmission of radiation through coniferous canopies, which cover vast areas of the boreal and temperate zones and play a major role in the global carbon cycle.

§12. Concluding remarks.

We have established in this chapter the fundamental structural variables—leaf area density and the leaf normal orientation distribution—that characterize the vegetation canopy within the turbid medium framework. The leaf area density, integrated vertically, yields the leaf area index; the leaf normal orientation distribution decomposes naturally into inclination and azimuthal components, each admitting several canonical analytical forms. The special case of needle canopies has been noted, requiring as it does a modified treatment of the projection geometry.

These structural variables are not mere abstractions. They may be estimated from field measurements, from lidar scanning, or from satellite observations of surface reflectance. The global maps of leaf area index derived from MODIS illustrate the power of remote sensing to provide these quantities over the entire terrestrial surface. In the chapters that follow, we shall employ these structural descriptions as the foundation for physical models of radiative transfer through vegetation canopies.